Polym. Bull. (2012) 68:2145–2174
DOI 10.1007/s00289-012-0721-2

ORIGINAL PAPER

The influence of additive property on performance of organic bulk heterojunction solar cells

Jiangang Liu · Yanchun Han

Received: 1 October 2011 / Revised: 18 January 2012 / Accepted: 18 February 2012 /
Published online: 24 March 2012
© Springer-Verlag 2012

Abstract The performance of bulk heterojunction organic solar cells based upon blends of donor and acceptor materials has been shown to be highly dependent on the microstructure and photoelectric properties of active layer. Recently, various methods, such as post-annealing, microwave annealing and control in the film-forming rate, and so on, have been used to modify the morphology to achieve high device performance. Among these methods, adding additives is a simple and promising approach, which can not only control the morphology but also improve the photon absorption or energy-level distribution of the active layer. In this review, we will introduce the additives that used widely in recent from following aspects: species, mechanism, and performance. First, the additive species and its selection principle according to special donor and acceptor system will be concluded. Then, the mechanisms of improved morphology and photoelectric properties by adding different kinds of additives will be illustrated in brief. At last, we will discuss the influences of additives on device performance.

Keywords Solar cells · Additive · Polythiophene · Crystallinity · Phase separation

Introduction

Solar cells have recently emerged as promising solar energy technologies [1]. Among these technologies, organic solar cells (OSCs) have received much attention because they have potential advantages, such as mechanical flexibility, light weight, and low cost [2]. Furthermore, organic semiconductor thin films show

---

J. Liu · Y. Han (✉)
State Key Laboratory of Polymer Physics and Chemistry, Changchun Institute of Applied Chemistry, Chinese Academy of Sciences, 5625 Renmin Street, Changchun 130022, People's Republic of China
e-mail: ychan@ciac.jl.cn

high absorption coefficients exceeding 10^5 cm^{-1} and high charge carrier mobilities [3, 4]. The electronic band gap of organic semiconductors also could be engineered by chemical synthesis [5]. Recently, devices that based on organic materials develop rapidly, the highest power conversion efficiency (PCE) for small-area OSCs approach to 8.0% [6–8], which is close to the large-scale commercial applications.

The architecture of solar cells has a profound influence on the device performance. Science, the seminal work of Tang [9], have undergone a gradual evolution from the single-layer to the donor/acceptor bilayer heterojunction and then to the donor/acceptor bulk heterojunction (BHJ). In single-layer organic solar cells, the pure conjugated polymer is sandwiched by electrodes with different work functions [10]. Due to the absence of donor/acceptor interface, the predominant tendency in the device is to form bound excitons that decay rather than dissociate, which results in a low short-circuit current (J_{sc}) and limits the PCE [11, 12]. To solve the problem, a two-layer organic solar cell was fabricated from copper phthalocyanine (CuPc) and a perylene tetracarboxylic derivative (PV) [9, 13]. This two-layer architecture led to improved exciton dissociation at the interface and efficient transport of carriers. However, the exciton diffusion length of typical organic materials is relatively small, on the order of 10 nm or so [14, 15]. As a result, only excitons generated near the donor/acceptor interface could dissociate, while the majority of the excitons created away from the interface also suffer from recombination [16].

To increase the efficiency of exciton dissociation, large internal interfacial area between donor and acceptor is necessary. Yu and Heeger [17] and Halls et al. [18] independently fabricated a so-called BHJ, which contains small donor and acceptor domains on nanoscale and has lots of interfacial area. In the BHJ, nearly all excitons could reach the donor/acceptor interface and are split into holes and electrons before recombining. Free holes and electrons then transport through the continuous percolation pathways to their respective electrodes.

As we know, in BHJ organic solar cells, the working principles include four steps: photon absorption and exciton generation; exciton diffusion and dissociation at donor/acceptor interface; carrier transport to respective electrodes; carrier collection by the electrodes [19–21]. To satisfy the requirement mentioned above, an idea BHJ should meet the following criteria:

1. Local molecular ordering and crystallinity should be high to ensure photon absorption, exciton transport, and charge transport;
2. Domain size of donor and acceptor should be proper (usually 10–20 nm) to ensure exciton dissociation and charge separation and transport;
3. Continuous percolation pathway and vertical segregation should be formed to ensure charge transport and collection.

To obtain a high device performance, it is necessary to carefully optimize the morphology of active layer. Recently, some approaches controlling the film morphology of BHJ solar cells have been reported, including adjusting the rate of film-forming process [22], control of cosolvent [23, 24], solvent annealing [25, 26], microwave annealing [27], and thermal annealing [28–30]. Although the local ordering and crystallinity and bicontinuous structure could be obtained [31, 32], it is challenging to apply these methods to practical fabrications. For example, thermal annealing is not compatible with the use of flexible substrates with low glass transition temperature, the solvent vapor annealing is not suitable for real roll-to-roll process for the dangers of solvent vapor [33, 34] and the cosolvent method tends to promote polymer chains to accumulate and form crystalline aggregates in solution, which shortens the solution shelf lifetime [35]. Moreover, the approaches mentioned above mainly focus on the morphology of active layers, while have little contribution on the improvement of the photons absorption as well as the energy distribution. As we know, these are also key factors to further improve the device performance.

It is necessary to create new procedure for the development of flexible low-cost OSCs with high performance. Since the first report on the addition of nanoparicles to improve the BHJ device performance by Carroll and coworkers [36], the concept of incorporation of other solvents, nanoparticles, small molecules, or polymers into the donor/acceptor blend system has been developed as an additive method. Additives play different roles according to its property as following: changing film-forming kinetics to improve the morphology of active layer; increasing the planarity of conjugated molecule or acting as nucleating agent; adjusting the interaction between donor and acceptor to control the scale of phase separation; changing the distribution of energy level at the donor/acceptor interface to increase open circuit voltage (V_{oc}); acting as sensitizer to widen the absorption spectrum. The additive method is a simple and promising approach. It is possible to select proper kind of additive according to the requirement of BHJ system and obtain a high device performance. In the following, we will introduce several kinds of additives according to their functions and discuss the influences on device performance, at the same time, the mechanisms are also illustrated in brief.

Species of additive and its selection principle

The volatile solvents, such as alkanethiol, are usually used as additives to modify the film morphology. They have a positive influence on device performance and could be removed after drying the film [37]. While some non-volatile materials which still retain in the film after film-forming process, also can act as additive to adjust the thermodynamically stable state or photoelectric properties of active layers. The energy level and carrier mobility of non-volatile additives have profound influences on device performance; as a result, it is necessary to select the additive elaborately according to the requirement of blend system.

Alkanethiol and diiodoalkane molecules

Recently, researchers present a method comprising the addition of alkanethiol and diiodoalkane molecules as processing additive to polymer/fullerene solution prior to spin-coating to improve the film-forming process [38–42]. During the film-forming, the changed thermodynamic and kinetic parameters, such as polymer state in solution, solvent vapor pressure, and solubility of solutes [39, 43] can enhance crystallinity of polymer, aggregation of fullerene, and affect vertical phase separation of active layer. Thus, it is feasible to adjust the morphology by changing the film-forming process.

To be a qualified additive, it must be mutually soluble with the host solvent to ensure a homogeneous film. After the mixture, the mixed solvents should reduce the entanglement of polymer chains in solution to facilitate its self-organization. Moreover, additives should not react with either the polymer or the fullerene and have a discrepancy in solubility between polymer and fullerene. The discrepancy in solubility would change the film-forming kinetic during the process of liquid–liquid phase separation and drying. For example, in poly[2,6-(4,4-bis-(2-ethylhexyl)-4H-cyclopenta[2,1-*b*;3,4-*b*′]-dithiophene)-alt-4,7-(2,1,3-benzothiadiazole)] (PCPDTBT)/$PC_{71}BM$ system, the diiodoalkane selectively dissolves the $PC_{71}BM$, but PCPDTBT is not soluble in diiodoalkane. As a result, three phases including a fullerene-diiodoalkane phase, a polymer aggregate phase, and a polymer-fullerene phase forms as shown in Fig. 1A [37], which is crucial to the final phase separation and crystallinity of polymer. In addition, the boiling point of the additive should be higher than the host solvent. Thus, it can prolong the film-forming process then provide adequate time for polymer to self-organize, which is similar to solvent annealing treatment [22, 44]. To achieve a suitable degree of phase separation, the boiling point should be adjusted according to solubility parameter difference between the additive and fullerene [45], which will be discussed exhaustively in the following.

In conclusion, in order to achieve an optimum morphology, the additive must come up to some of the following criteria: (i) reduce the polymer chains entanglement in solution, (ii) have a discrepancy in solubility between polymer and fullerene, (iii) have a higher boiling point than host solvent (the boiling point should be adjusted according to solubility parameter difference between the additive and fullerene).

Aromatic ring molecule and nucleating agent

The crystallinity of polymer in polymer/fullerene blends system is crucial to the device performance, concerning with the photons absorption and charge transport. As is well known, the crystallization of P3HT is driven by a single chain mechanism. A coil-to-rod transformation in P3HT main chain conformation followed by interchain π–π stacking is thought to be the precondition toward crystallization [46]. Consequently, rod-like rigid conformation of P3HT chains is quite necessary for production of P3HT crystals. However, the chains entanglement certainly hinders its coil-to-rod transformation [47]. While some aromatic ring and nucleating agent could aid P3HT chains adopt rod-like rigid conformation and result in high crystallinity.

Such as a perfluorinated compound, 4-amino-2-(trifluoromethyl)benzonitrile (ATMB) [48], the P3HT monomer 3-hexylthiophene (3HT) [34], and so on [49] can be used as additive to improve the conformation of polymer chains. The improved conformation could enhance the intra- and interplane stacking of P3HT chains, which result in a high crystallinity. The crystallinity of conjugated polymers could also be controlled by introducing crystallization nucleating agent. These additives acting as nucleating agent usually have a strong chemical affinity toward polymer.

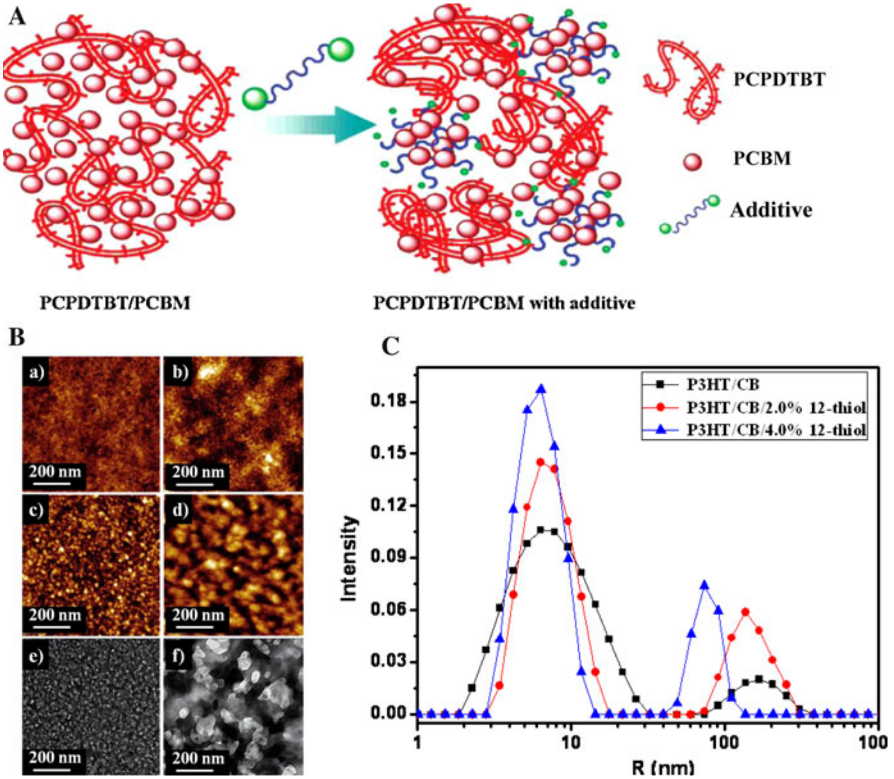

Fig. 1 **A** Schematic depiction of the role of the processing additive in the self-assembly of BHJ blend materials. **B** AFM and TEM images of BHJ films cast from PCPCTBT/PC$_{71}$BM without and with ODT and exposed PCPDTBT networks after removal of PC$_{71}$BM in BHJ film; AFM image of BHJ film (*a*) without and (*b*) with ODT; AFM image of exposed polymer networks (*c*) without and (*d*) with ODT; and TEM image of exposed polymer networks (*e*) without and (*f*) with ODT. Reproduced with permission from Ref. [37]. **C** DLS spectra for P3HT/chlorobenzene solutions with different volume fraction of *n*-dodecylthiol. Reproduced with permission from Ref. [40]

Sometimes their difference of lattice periodicity should be smaller than 15% [50, 51]. Researchers introduced a copolymer based on thieno[3,2-*b*]thiophene and pentathiophene units (DHPT^3) [52] or oleic acid (OA) [53] to P3HT/PCBM BHJ photovoltaic devices. Due to the pronounced molecular planarity of thienothiophenes and/or the strong chemical affinity of pentathiophene toward P3HT, the additive act as crystallization nucleating agent in this blend system. The interaction between the copolymer and P3HT molecules induces a marked structural ordering of the polythiophene phase.

According to the function of additive, to improve the crystallinity of polymers, the additive must come up to some of the following criteria: (i) the additive acting as nucleating agent usually has a strong chemical affinity toward polymer; (ii) to enhance the coplanar conformation of polymer chains, the additive must have a strong interaction with the polymer.

Hydrophobic and amphiphilic molecules

As mentioned above, the phase separation can be drove by crystallization of polymer or changed film-forming kinetics. Unlike the previous methods, incorporation of additives to alter the interaction parameter between electron donor and acceptor is also an effective approach to control the morphology. Increasing the incompatibility between donor and acceptor could obtain a large phase separation, while increasing the compatibility could gain a thermodynamically stable nanoscale morphology.

In P3HT/$PC_{61}BM$ blend system, inducing hydrophilic–hydrophobic repulsive interaction in boundaries between the relatively hydrophilic PCBM and the relatively hydrophobic P3HT could increase the phase separation. As a result, the hydrophobic material, such as transition metal complexes, organic salt as shown in Fig. 3A [54] and some functionalized polymer, like hydrophobic end-functionalized P3HT (F-P3HT) [55] are all good candidates to act as this kind of additive. It is obvious that the additive is preferentially segregated in P3HT domains, because of the relatively hydrophobic P3HT. As a consequence, the hydrophilic–hydrophobic repulsive interaction between P3HT and PCBM increases, which results in an enhanced extent of phase separation.

Some of active layer structures are kinetically trapped, thus further coarsening of the phase-separated domains is inevitable due to heat generated during continued device operation [56, 57]. This coarsening in turn reduces the density of the heterojunction interface available for exciton dissociation; devices under extended operation thus exhibit characteristics that deteriorate with time [58]. To prevent the coarsening of the phase-separated domains upon operation process or thermal annealing, the additives, block copolymers, which comprise electron donor and electron acceptor segments have been employed as photoactive layers in OSCs [59, 60]. These additives generally reside at the interface between electron donor and acceptor to minimize unfavorable enthalpic contacts, leading to a thermodynamically stable nanoscale morphology. Recently, Sivula et al. have demonstrated the synthesis of a well-defined donor–acceptor amphiphilic diblock copolymer, poly(**1**)-*block*-poly(**2**) (as shown in Fig. 4A), by using ring-opening metathesis polymerization (ROMP). The diblock copolymer contains a C_{60}-containing monomer (1) and an end-functionalized P3HT macromonomer (2), which increases the compatibility between P3HT and $PC_{61}BM$. It plays a critical role in tuning the morphology of active layer when employed as additive, leading to stabilization of the device structure against destructive thermal phase segregation [61]. However, the J_{sc} of these devices are lower than those initially exhibited by the uncompatibilized, reference devices. This reduction is attributed to the presence of large insulating groups or saturated hydrocarbon backbones in these block copolymers, which ultimately hinder charge separation and transport at the donor/acceptor interface [58, 62, 63]. To avoid the influence of insulating groups, Kim et al. [58] chosen to evaluate solution-processable small molecule donor–acceptor dyads, thiophene-C_{60} dyads (designated 4T-C_{60}, where 4 represents the number of thiophene units attached to the fullerene), with minimal insulating linker in between the electrically active moieties as potential compatibilizers for P3HT and PCBM. As a result, both the thermal stability and electrical property are preserved.

In conclusion, incorporation of additives to alter the interaction parameter between electron donor and acceptor is an effective approach to control the degree of phase separation. To increase the domain size, additives, usually a hydrophobic end-functionalized donor or a hydrophilic end-functionalized acceptor, should induce a hydrophilic–hydrophobic repulsive interaction in the boundary between donor and acceptor. To obtain a thermodynamically stable nanoscale morphology, the donor–acceptor amphiphilic diblock copolymer with small insulating groups should be used, which minimize unfavorable enthalpic contacts between the electron donor and acceptor.

Sensitizer and metal nanoparticles

In addition to morphology of active layer, the light absorption is also an important factor for high performance device. For example, in P3HT/PCBM system, the PCE is limited as high as 5% due to the insufficient light absorption by P3HT (caused by a mismatch of its band gap, 2.2 eV, with the photon flux maximum of the solar spectrum at the standard air mass 1.5 conditions, which lies between 1.3 and 2.0 eV) [64]. Further improvement of polymer solar cells requires active layer to absorb broader and longer wavelength to match the terrestrial solar radiation. To improve the light absorption, new electron donor [8, 65] and acceptor materials [52, 66] and device architectures [67, 68] have been developed by different research groups. However, adding additive to complement absorption spectra of active layer is a simple and effective method to increase the photon absorption. This kind of additives can be divided into three categories: the additives that complement absorption spectra of active layer, the additives that have energy transfer to electron donor or acceptor and act as sensitizer; the metal nanoparticles that reflect and scatter light to increase the optical path.

The additives that complement absorption spectra of active layer, such as SM [69], SMD1 [70], and tetramethyl-substituted copper (II) phthalocyanine (CuMePc) nanocrystals [71] have a matched energy level and complementary absorption spectra with P3HT and fullerene. For example, SM is a small molecule containing thienothiadiazole central unit with terminal cyanovinylene 4-nitrophenyl at both sides and exhibits a wide absorption band in the wavelength region of 580–680 nm, which result in almost the entire visible spectrum absorption as blended with P3HT and $PC_{61}BM$, as shown in Fig. 5A. The HOMO and LUMO levels of SM are 5.15 and 3.45 eV, respectively, lying between the energy levels of P3HT (HOMO is 5.0 eV, LUMO is 3.10 eV) and $PC_{61}BM$ (HOMO is 6.2 eV, LUMO is 3.90 eV). As a result, photogenerated excitons might be dissociated efficiently at P3HT/SM, P3HT/$PC_{61}BM$, and SM/$PC_{61}BM$ interfaces and carriers also can be effectively transport to respective electrodes [69].

The additive also can be act as sensitizer to enhance the absorption of acceptor or donor. As we know, the common electron acceptor, $PC_{61}BM$, has outstanding electron conduction property, but shows only little absorbance in visible wavelength range [72]. Although the alternative electron acceptors, such as vinazene, perylene, and quinine [73–75], show enhanced light absorption with respect to fullerenes, bimolecular recombination occurs in these systems and limits charge collection efficiencies [76]. While the sensitizer for $PC_{61}BM$, such as 2,9-di(pent-3-yl)-anthra [2,1,9-def:6,5,10-d′e′f′] diisoquinoline-1,3,8,10-tetrone (PDI), could be used to make up for the weak photon absorption of $PC_{61}BM$. There is energy transfer from photoexcited PDI molecules to $PC_{61}BM$, which results in strongly increased light harvesting of $PC_{61}BM$ and leads to improved light harvesting and current generation [77]. In addition to adding sensitizer for electron acceptor, introduction of sensitizer for electron donor is also an effective method to increase the optical absorption. Silicon phthalocyanine derivative (SiPc) can be used as sensitizer for P3HT:PCBM system [78], because of long-range Förster energy transfer energy transfer from P3HT to SiPc. The efficient long-range Förster energy transfer can increase exciton diffusion length, leading to an efficient dissociation of excitons from P3HT. Furthermore, extra photon absorption at about 650–700 nm of the incorporated SiPc itself also has a direct contribution to device performance. Furthermore, a suit energy level of sensitizer is also important for a qualified additive. In P3HT:$PC_{61}BM$:SiPc system, the energy level of SiPc lies between P3HT and $PC_{61}BM$, which ensures injection of electrons into $PC_{61}BM$ and holes into P3HT at the donor/acceptor interface. While in the case of polymer:$PC_{61}BM$:PDI system, the HOMO (LUMO) of PDI is lower (higher) than the corresponding energy of $PC_{61}BM$. As a result, the sensitizer remains electrically neutral when energy transfer occurs from the photoexcited dye to the fullerene. This process is therefore not significantly influence the charge recombination and transport kinetics.

As we know, metal nanoparticles exhibit localized surface plasmon resonances (LSPR) that couple strongly to the incident light. In addition, relatively large metallic nanoparticles can reflect and scatter light and thereby increase the optical path length within the active layer [36, 79]. As a result, adding nanoparticles to BHJ offers the possibility of enhanced absorption. Moreover, the work function of nanoparticles should be close to the HOMO energy level of P3HT, this could result in a small energy barrier for hole extraction. For example, the usage of large Au nanoparticles (about 70 nm) might lead to a reduced series resistance, because the holes need to pass through fewer interfaces than in the system with small Au nanoparticles as shown in Fig. 5C. Recently, moderate increases in PCE through the addition of metal nanoparticles have been reported [36, 79, 80].

Incorporation of additives to increase the photoabsorption is a simple and promising method to improve the device performance. We can use additives with complementary absorption spectra of active layer to widen the spectrum absorption range. If the donor or acceptor has poor absorption spectra, the sensitizer leading a stronger light harvesting through the energy transfer could be employed. In addition, the metal nanoparticles are also effective additives, nanoparticles with proper diameter and work function could enhance light absorption and reduce series resistance.

Liquid crystal molecules and others

Broad photon absorption, higher charge carrier mobility, and suitable electronic energy levels of both donor and acceptor materials are crucial for high-efficiency OSCs [81]. In addition to increasing the J_{sc} as mentioned above, there is still plenty of room to improve the efficiency of BHJ photovoltaic cell by improving the V_{oc}. As we know, the V_{oc} of a BHJ solar cell can be estimated by the following formula [82]:

$$V_{oc} = (1/e)\left(|E^{Donor}\mathrm{HOMO}| - |E^{Acceptor}\mathrm{LUMO}|\right) - 0.3\ \mathrm{V}$$

In order to further improve the open circuit voltage of the OSCs, lots of works have been attracted for optimizing the electronic match between donor and acceptor component by designing new donor or acceptor [66, 73, 83].

Exhilaratingly, Jeong et al. [84] found a simple approach to avoid the tedious synthetic experiment to adjust open circuit voltage. They incorporated a small portion of discotic liquid crystal, 2,3,6,7,10,11-hexaacetoxytriphenylene (DLC) into P3HT/$PC_{61}BM$ blend system as additive, which has a strong self-assembling ability and high mobility. After the addition of DLC, an average PCE = 3.97% is achieved after thermal annealing, compared to the reference cells with PCE = 3.03%. Besides the DLC, nematic liquid crystals, 4-cyano-4′-pentylbiphenyl (5CB) and 4-cyano-4′-octylbiphenyl (8CB) (NLCs) [85], (*S*)-5-octyloxy-2-[4-(2-methylbuthoxy)-phenylimino-methyl]-phenol (LC) [86] and n-type perylene derivative, *N*,*N*'-bis-(5-bromopyridine-2-yl)-1,6,7,12-tetrakis(4-*n*-butoxyphenoxy)-3,4,9,10-perylene tetracarboxycliimide (PPyB) [87] are also applied to OSCs as additives to increase the V_{oc}. One plausible reason for this result might be the changed energy-level distribution after adding the additives. In active layer, a cascade energy-level alignment is established, since the additives exhibit a lower-lying HOMO level compared to P3HT. This larger energy difference ($|E^{additive}\mathrm{HOMO}| - |E^{PCBM}\mathrm{LUMO}|$) between the additives and $PC_{61}BM$ may contribute to the increased V_{oc}. In addition, liquid crystals were reported to have unique one-dimensional charge carrier ability through the columnar axis when self-assembled in hexagonal columnar mesophases. The charge mobility of columnar-packed DLCs exhibits up to 0.5–1.0 $cm^2/V\ s$ compared favorably to that of amorphous silicon [88]. The higher mobility could play an important role in increasing charge transport in the active layer, contributing to the high current density of OSCs. Moreover, the additives also induce improved crystallinity of P3HT chains, even though the ordering of P3HT chains is hampered by the presence of $PC_{61}BM$ aggregates [84] (Table 1).

In conclusion, the energy-level distribution of the additive is a crucial criterion, which should have cascades in both LUMO and HOMO levels between electron donor and acceptor. Moreover, the additive should have a strong self-assembling ability, which induces the polymer to form more ordering structure.

The mechanisms of improved performance by adding additive

To improve the device performance, different kinds of additives play different roles. According to species of additive, the mechanism that additives optimize the device performance can be conclude as following: changing film-forming kinetics, increasing the planarity of conjugated molecule or acting as nucleating agent, adjusting the interaction between donor and acceptor to control the scale of phase separation, changing the distribution of energy level of active layer, acting as sensitizer to widen the absorption spectrum, and so on.

Table 1 Chemical structures of part of additives mentioned in this paper

Additive	Structure
Alkanethiol and diiodoalkane	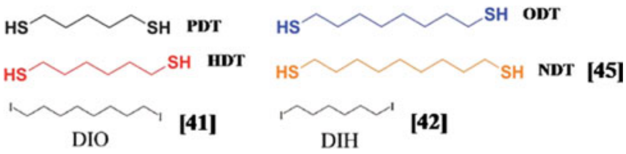 PDT ODT HDT NDT [45] DIO [41] DIH [42]
Aromatic ring molecule and nucleating agent	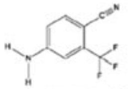 **ATMB [48]** 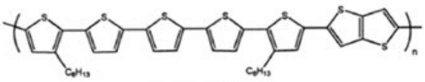 **DHPT^3 [52]**
Hydrophobic molecule	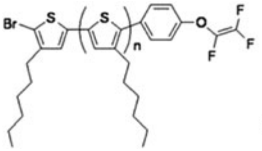 **F-P3HT [55]**
Amphiphilic molecule	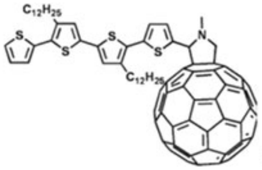 **4T-C$_{60}$ [58]**
Sensitizer and metal nanoparticles	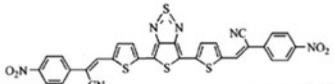 **SM [69]** 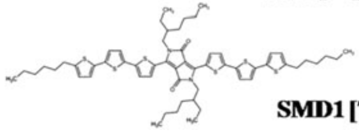 **SMD1 [70]** 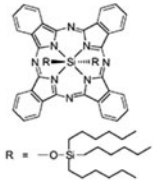 **SiPc [78]**
Liquid crystal molecules and others	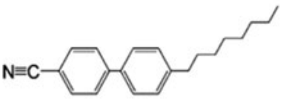 **NLC (8CB) [85]** 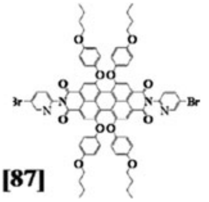 **PPyB [87]**

Change solution state and film-forming kinetics

Using alkanethiol and diiodoalkane as additives can reduce the entanglement among polymers, prolong the film-forming time and change the sequence of solute precipitation due to its low vapor pressure and selective solubility. The changed film-forming process improves the self-organizing ability of polymer and enhances the degree of phase separation, which is benefit for constructing a bicontinuous interpenetrating network.

In P3HT/$PC_{61}BM$ system, the crystallinity of P3HT and the phase separation are all improved after the addition of alkanethiol [40]. Bazan et al. employed the GIXD to prove the evolution of well ordered P3HT crystallites. Adding the alkanethiol, the intensity of P3HT diffraction peak increases, which indicates an enhanced crystallinity of P3HT. Moreover, the decreased width at half maximum of the diffraction peak obtained from the thiol-processed samples also suggests an enlarged P3HT crystalline domains. The improved crystallinity of P3HT is attributed to the enhanced P3HT self-organization ability, which can be confirmed by the more pronounced vibronic peaks in UV–Vis absorption spectra [40]. The addition of additive also enhances the phase separation between donor and acceptor. From the AFM height and phase images, significantly rougher surfaces and PCBM clusters in the film could be clearly observed after adding the additive [39, 40], which indicate an enhanced phase separation. The additive is also effective in other system, such as in PCPDTBT/$PC_{71}BM$ blend system [37]. When the diiodoalkane is added into the active layer, more elongated fibril-like domains and larger scale phase separation than that in the BHJ film made without any processing additive are observed. The fibril-like domains formed polymer network as shown in Fig. 1B, which can be confirmed by selectively dissolving out the fullerene from BHJ composite films. The network would improve charge transport.

The evolution of microstructure can be explained by the fact that the additive changes the aggregate state of polymers in solution and the film-forming kinetics during the drying process. In P3HT:PCBM system, *n*-dodecylthiol has an influence on the aggregate state of P3HT in solution. After the addition of *n*-dodecylthiol, the entanglements among P3HT chains become disentangled. Some of P3HT chains escape from the amorphous aggregates and randomly distribute as single molecules or smaller aggregates in the solution, which can be confirmed by the dynamic light scattering (DLS) results as shown in Fig. 1C. As a result, P3HT single chains gain more freedom in rotation or motion, which improves the P3HT self-organized ability and thus is benefit for its crystallization [40]. During the film-forming process, the additive prolongs the film-forming time and changes the sequence of solute precipitation due to its low vapor pressure and selective solubility. This allows additives to interact with polymer or fullerene component after the evaporation of host solvent and provide adequate time for polymers to self-organize, which is similar to solvent annealing treatment [22]. In addition, the additive selectively dissolves the fullerene or polymer component [37, 39]. As the host solvent evaporates, one component in solution would precipitate prior to the other one and formed aggregates due to the limited solubility in additive. As a result, the polymers could self-organize without the disturbance of fullerene, then a higher crystallinity would be achieved. The extent of phase separation correlated mainly to the degree of intermolecular interactions between the additive molecules and the solute and the drying time of the film. Salim et al. investigated the influence of solubility parameter (δ) and boiling point (T_b) on extent of fullerene aggregation.

Solubility parameter is employed to estimate the interaction strength between additive and fullerene molecule [45]. Two molecules are considered to have good interaction if the solubility parameter difference ($\Delta\delta$) between them is small. They have systematically investigated the effect of alkanedithiols with different alkyl chain lengths on the morphology of P3HT:$PC_{61}BM$ BHJ. Both the boiling point (T_b) and solubility parameter of the additives are important parameters, which should be considered simultaneously. Among the additives including 1,5-pentanedithiol (PDT), 1,6-hexanedithiol (HDT), 1,8-octanedithiol (ODT), and 1,9-nonanedithiol (NDT), the PDT and NDT favor $PC_{61}BM$ to aggregate. Although $\Delta\delta$ between NDT and $PC_{61}BM$ is the smallest, its high T_b prolongs film-forming process, which provides sufficient time for NDT to interact with $PC_{61}BM$ and then forms larger fullerene aggregates. Conversely, PDT has the lowest T_b, but gives the largest $\Delta\delta$, and it also enhances the aggregation of $PC_{61}BM$. It suggests that the poor interaction between two molecules could promote the fullerene to aggregate. So, it is necessary to carefully modulate the choice of both δ and T_b of the additive to optimize blend morphology when the additive molecules are incorporated into the blend.

Not only the crystallinity and aggregation size but also the vertical phase separation could be influenced by adding the additive. In P3HT/$PC_{61}BM$ blend system, the distribution of P3HT in the vertical direction is homogeneous when PEDOT:PSS-coated ITO is used as the substrate. However, in the mixture solvent with additive, P3HT ratio for the top surface is higher than that of the bottom, suggesting P3HT-enriched region in the surface and depleted region in the bottom [39]. The fact that the additive prolongs the film-forming process, and provides adequate time for molecule migration. As a result, higher surface energy of PCBM than P3HT may lead to rich PCBM distribution at the bottom of active layer. However, this situation would not be expected for better charge collection when PEDOT:PSS-coated ITO is used as substrates. The observed vertical phase separation makes it ideal for an inverted solar cell structure.

It is obvious that the addition of additive to change solution state and film-forming kinetics has a profound influence on film morphology: in solution, the additive reduces the polymer chains entanglement and favors its self-organization; during the film-forming process, the disturbance of fullerene is restricted which facilitates the polymer crystallization; moreover, the prolonged film-forming process and poor interactions between fullerene and additives is benefit for the phase separation. As a result, an optimized morphology of blended film is obtained, resulting in an improved device performance.

Enhance the self-organized ability of polymer chains

The self-organized ability of polymer chains could be enhanced by adding aromatic ring molecules or nucleating agent, such as ATMB, 3HT, OA, and so on. The improved crystallinity results from the enhanced coplanar conformation of polymer chains and extra induced nucleating agent.

After addition of aromatic ring molecules, such as ATMB, 3HT, the self-organized ability of polymer chains could be enhanced. When compared with the pristine P3HT:PCBM blend film, the film with additive exhibits a higher absorbance

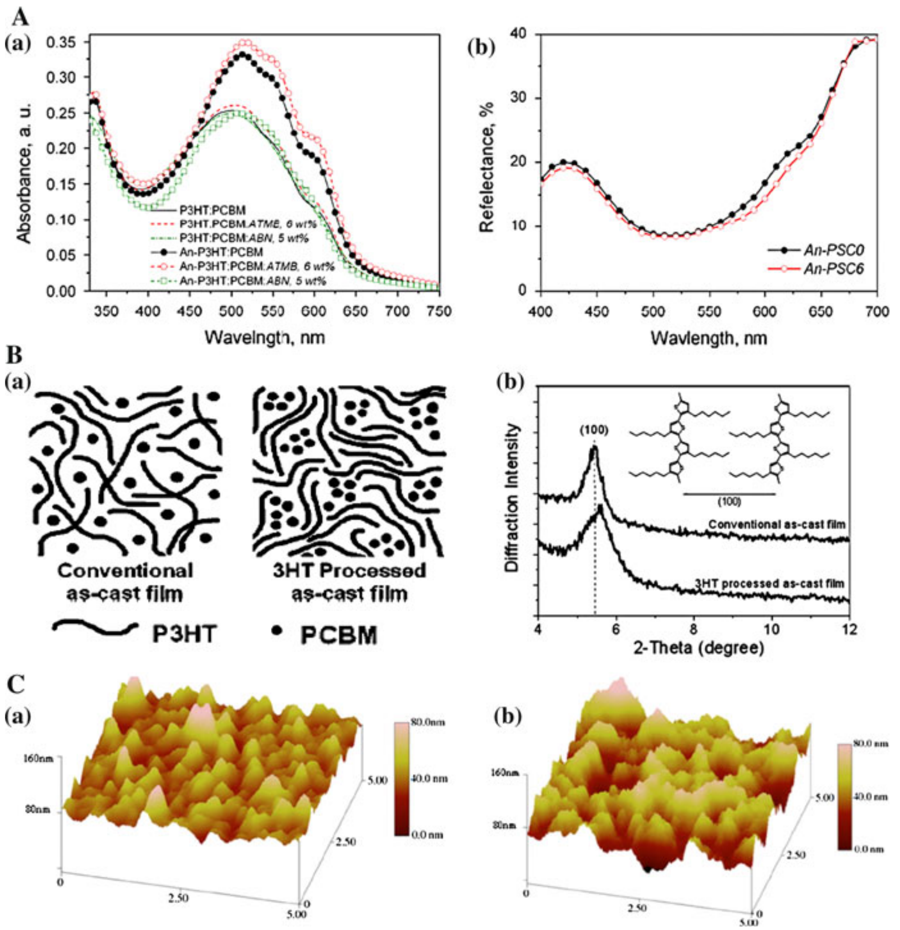

Fig. 2 **A** UV–visible absorption spectra of the P3HT:PCBM blend films with and without additives (*a*) and reflectance spectra of annealed devices (*b*). Reproduced with permission from Ref. [48]. **B** (*a*) Schematic representation of the morphologies of P3HT/PCBM films prepared by various processes. (*b*) XRD profiles of P3HT/PCBM films fabricated from the P3HT/PCBM/chlorobenzene solutions with and without addition of 3-hexylthiophene. Reproduced with permission from Ref. [34]. **C** AFM images, showing the surface morphology of the photovoltaic films of P3HT:PCBM:OA without (rms = 8.84 nm) (*a*) and with OA (rms = 12.39 nm) (*b*) after annealing (image size 5 × 5 μm^2). Reproduced with permission from Ref. [89]

in major absorption peak (520 nm) of π–π* transition and two vibronic peaks of 550 and 600 nm (as shown in Fig. 2A). At the same, the reflectance of the annealed devices with additive reduces in visible region is shown in Fig. 2A. All these indicate an enhanced self-organized ability of P3HT. At the same time, the crystal number increases and its size is also larger compared with that of the pristine film. In addition to the crystallinity, the crystal structure changed after adding the 3HT. X-ray diffraction (XRD) data reveal a smaller interlayer distance between conjugated backbones in the 3HT-processed film as shown in Fig. 2B(b). According to Bragg's equation, the 3HT-processed film has a mean interlayer spacing of

15.7 Å, which is 1.4 Å less than that of the reference film (16.3 Å). These results clearly indicate that incorporating a tiny amount of additive into solution enhanced the intra- and interplane stacking of P3HT chains in the as-cast P3HT/PCBM films, forming a highly ordered structure.

Introducing crystallization nucleating agent could also enhance the crystallinity of conjugated polymers. The additive acting as nucleating agent usually has a strong chemical affinity toward polymer and sometimes their difference of lattice periodicity should be smaller than 15% [50, 51]. Bechara et al. [52] introduced $DHPT^3$ to P3HT/PCBM BHJ photovoltaic devices. Due to pronounced molecular planarity of thienothiophenes and strong chemical affinity of pentathiophene toward P3HT, the $DHPT^3$ acts as crystallization nucleating agent in P3HT/$PC_{61}BM$ blend system. The interaction between copolymer and P3HT molecules induces a marked structural ordering of the polythiophene phase. The scale of phase separation is also improved which is drove by the improved crystallization process as shown in Fig. 2B(a) [89]. During the film-forming process, the OA may induce a better ordering or form more crystalline nucleus in the as-prepared film, which results in a high crystallinity of P3HT after the thermal annealing. While in P3HT/PCBM composite film, $PC_{61}BM$ resides only in the amorphous P3HT domains [53]. The enhanced P3HT crystallinity decreases the solubility of $PC_{61}BM$ in it, which results in a large scale of phase separation and continuous electron pathways. This is confirmed by the increased roughnesses of AFM images as shown in Fig. 2C.

Adding aromatic ring molecule or nucleating agent is a promising method to improve the morphology of active layer. The rigid conformation of polymer could be induced by the additives, which results in an enhanced crystallinity. The degree of phase separation also increased, which is promoted by the crystallization of polymer in blend system.

Adjust the compatibility between donor and acceptor

The phase separation degree of active layer in BHJ has a profound influence on device performance. A fine phase separation would hinder charge transport; on the contrary, a large phase separation would be not benefit for dissociation of exciton. As a result, controlling the domain size and preventing further coarsening during continued device operation should be carefully considered. As we know, the degree of phase separation is dominated by the interaction parameter between donor and acceptor materials. Thus, adjusting the interaction parameter to control the phase separation represents a robust, reliable, and reproducible method for enhancing device efficiencies in BHJ solar cells.

The phase separation can be enhanced by introducing hydrophilic–hydrophobic repulsive interaction. Transition metal complexes and organic salt which have different hydrophobicity (as shown in Fig. 3B) are employed as additive to improve the morphology of P3HT/$PC_{61}BM$ inverted BHJ devices [54]. After the addition of additive, the phase separation characteristics of P3HT and $PC_{61}BM$ are enhanced, leading to the formation of more $PC_{61}BM$ clusters. Because of the relative hydrophobicity of P3HT compared with $PC_{61}BM$, the additive is preferentially segregated in P3HT domains. The selective incorporation enhances the interaction

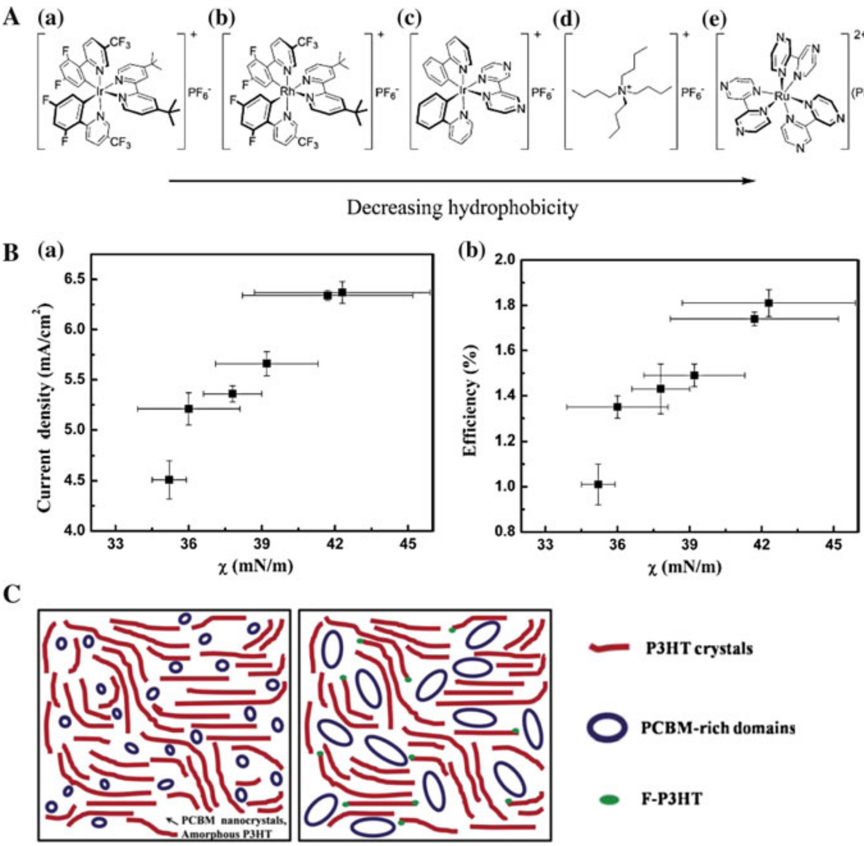

Fig. 3 **A** Molecular structures of additives used in this work. Their structures are listed with decreasing hydrophobicity of the surrounding ligands. **B** Device characteristics, including (*a*) short-circuit current and (*b*) device efficiency as a function of χ (mN/m), the interaction parameter between the electron donor and acceptor phases. Reproduced with permission from Ref. [54]. **C** Schematic illustration of a P3HT:PCBM blend film (*left*) and a P3HT:F-P3HT:PCBM blend film (*right*), hydrophobic F-P3HT induce phase separation with relatively hydrophilic PCBM preserving the crystallinity of P3HT. Reproduced with permission from Ref. [55]

parameter (χ is a measure of the extent of chemical incompatibility between two species) between P3HT and $PC_{61}BM$. As a result, the extent of phase separation is influenced by the hydrophobic additives, with the most hydrophobicity increasing phase separation the most. On the base of inducing hydrophilic–hydrophobic repulsive interactions in the boundary, Lim et al. [55] also synthesized a novel hydrophobic end-functionalized P3HT to preserve the crystallinity of P3HT. The additive not only leads to larger size $PC_{61}BM$ clusters but also improves the crystallinity of P3HT as illustrated in Fig. 3C, which provides a maximized continuous interfacial area and is benefit for the photon absorption and charge transport. In conclusion, the additive increasing the hydrophilic–hydrophobic repulsive interactions between donor and acceptor could enhance the scale of phase separation.

In contrary, the phase separation can be suppressed by decreasing the hydrophilic–hydrophobic repulsive interactions, that is to say, increasing the compatibility between donor and acceptor materials. The well-defined donor–acceptor amphiphilic diblock copolymer, such as poly(**1**)-*block*-poly(**2**), and small molecules, such as 4T-C_{60}, could act as the compatibilizers [58, 61]. The compatibilizers play a critical role in suppressing the macrophase separation and leading to a stable device structure [61]. As-cast films of P3HT:$PC_{61}BM$ show no phase segregation (as shown in Fig. 4A). Upon annealing the film at 140 °C, the blend constituents diffuse and aggregate into micrometer-scale features and these phase domains keep increasing in size with longer thermal treatment. After adding 5 wt% poly(**1**)-*block*-poly(**2**) to the blend film, there is no effect on the as-cast morphology. But subsequent annealing produces micrometer-order band-type features as shown in Fig. 4A, which indicates a reduction in surface tension between the growing $PC_{61}BM$ aggregates and the polymer film. While the addition of poly(**1**)-*block*-poly(**2**) up to 17 wt%, subsequent annealing has no effect on the phase separation and no detectable large domains are observed. Furthermore, the structure of additive should be elaborately designed. When employed thiophene-C60 derivatives, *n*T-C60 (where *n* represents the number of thiophene units attached to the fullerene), as additive for P3HT/$PC_{61}BM$ system, the number of thiophene units has a profound influence on the final morphology [58]. 4T-C60 is the most effective among the derivatives tested; its incorporation at 5 wt% to P3HT/$PC_{61}BM$ system effectively suppresses the macrophase separation, even upon extended thermal annealing. In sharp contrast to 4T-C60, the addition of 8T-C60 to active layers does not arrest macrophase separation on extended annealing, because its surface energy (16.8 mN/m) is comparable to that of P3HT (16.6 mN/m), then likely to be miscible with P3HT. In the case of 2T-C60, the thiophene segment is too short. Although 2T-C60 is still likely to reside at the interface between P3HT and $PC_{61}BM$, it cannot effectively increase interfacial adhesion and arrest domain coarsening as shown in Fig. 4 B(a).

The changed phase separation is induced by changed surface tension between the growing $PC_{61}BM$ aggregates and the polymer film. The hydrophobic or hydrophilic additives which selectively reside at one component could enhance the scale of phase separation by increasing the hydrophilic–hydrophobic repulsive interaction between donor and acceptor materials. The hydrophilic–hydrophobic additives which reside at the interface between donor and acceptor component could lower the surface energy to a point where no detectable phase segregation is observed after annealing.

Improve photon absorption of active layer

As we know, the OSCs based on polymer:$PC_{61}BM$ system are usually limited by the mismatch between the polymer absorption band and the solar spectrum. As a result, harvesting more photons through the addition of additives is an effective and simple way to improve the device performance [70].

The additives, such as SM [69], SMD1 [70], and tetramethyl-substituted copper (II) phthalocyanine (CuMePc) nanocrystals [71] are good candidates to improve

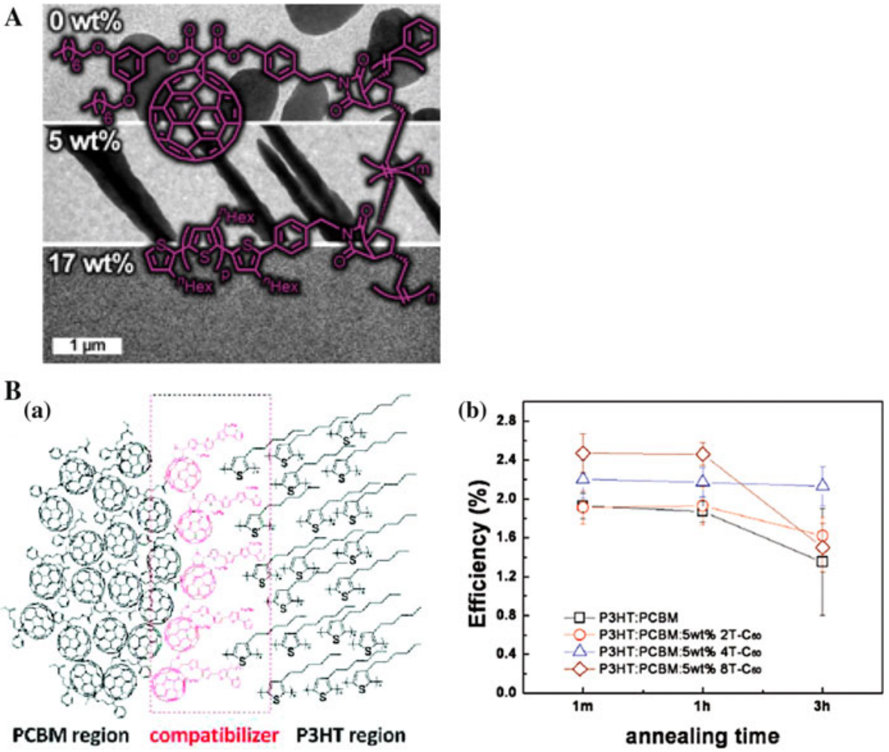

Fig. 4 **A** TEM image of a thin film of P3HT/PCBM blend before annealing (*upper*), and P3HT/PCBM + 5 wt% poly(**1**)-*block*-poly(**2**) after annealing (1 h, 140 °C) (*middle*), and P3HT/PCBM + 17 wt% poly(**1**)-*block*-poly(**2**) after annealing (1 h, 140 °C) (*lower*). Reproduced with permission from Ref. [61]. **B** (*a*) Schematic illustration of a P3HT:PCBM with 4T-C_{60} as compatibilizer. (*b*) Average efficiencies of P3HT:PCBM devices comprising 5 wt% 2T-C_{60}, 4T-C_{60}, and 8T-C_{60}. All devices were annealed at 170 °C under N_2 atmosphere. Reproduced with permission from Ref. [58]

photon absorption of P3HT/PCBM system, as they exhibit complementary absorption spectra compared with P3HT/PCBM films. In addition, the HOMO and LUMO levels of additives lie between the energy levels of donor and acceptor. So, photogenerated excitons could be dissociated efficiently at the interface and carriers also could be effectively transport to respective electrodes. Owing to the above advantages, the device performance is optimized by the addition of these additives.

In the case of sensitization of $PC_{61}BM$, using the PDI as sensitizer can improve its photon absorption, thus significantly enhanced photovoltaic performance [77]. Adding small amounts of PDI to $PC_{61}BM$ yields an increase emission from the fullerene, which is attributed to an energy transfer from the strongly absorbing perylene dye to the $PC_{61}BM$. Assuming a fluorescence yield of $\phi_F = 0.96$ and a refractive index of 1.5, a Förster radius of 2.8 nm for the PDI–$PC_{61}BM$ system can be estimated [90, 91]. Energy transfer from photoexcited PDI molecules to $PC_{61}BM$

is expected to result in strongly increased $PC_{61}BM$ triplet yield [92]. Based on the distribution of LUMO, electron transfer from PDI to $PC_{61}BM$ is also possible. The energy transfer followed by charge separation at the interface to the donor molecule. Thus, combining the strong absorption of PDI in the visible light and the outstanding properties of $PC_{61}BM$ as electron acceptor, which result in increased photon absorption and thus current generation.

Introducing the SiPc as sensitizer to P3HT is also an effective method to increase the light harvesting [78]. SiPc has two bulky groups in the axial direction perpendicular to the phthalocyanine plane, which probably suppress the formation of dye aggregations and is benefit for the effective absorption. In blend system, SiPc prefers to locate at P3HT/PCBM interface and fabricates energetic cascade in both LUMO and HOMO levels between P3HT and PCBM. After the addition of SiPc, the EQE corresponding to direct photoexcitation of SiPc (650–700 nm) is about 20%, while the EQE corresponding to the P3HT absorption increases from 50 to 60% after the addition of SiPc as shown in Fig. 5B. It suggests two origins for the increase in J_{sc} by the addition of SiPc molecules exist: One is that the direct contribution of SiPc to the photocurrent, which results from photoexcitation of SiPc itself. The other origin can be illustrated that SiPc molecules promote the charge separation from P3HT excitons at the interface. The phenomenon could be attributed to Förster energy transfer from P3HT to SiPc. Simple calculation assuming point dipoles gives a large Förster radius of beyond 3 nm for energy transfer from P3HT to SiPc. The energy transfer rate from P3HT to SiPc is estimated to be as fast as about $8 \times 10^{12}\ s^{-1}$ for a spatial separation of 1 nm, which is over a 100 times faster than the energy migration rate among P3HT at the same spatial separation. Therefore, the efficient long-range Förster energy transfer can collect P3HT excitons that could not reach the interface. The Förster energy transfer is not random diffusion but directional transports from a donor to an acceptor molecule. Thereby, the addition of SiPc can harvest P3HT donor excitons more efficiently into the SiPc acceptor at the interface, as shown in Fig. 5B.

Adding metal nanoparticles as additive to BHJ films offers the possibility of enhanced absorption and a reduced series resistance of the active layer. Wang et al. [79] mixed truncated octahedral Au nanoparticles into active layers of P3HT:$PC_{71}BM$, PCDTBT: $PC_{71}BM$, and Si-PCPDTBT: $PC_{71}BM$ system directly. After the addition of Au nanoparticles with diameter about 70 nm, all the systems show improved device performances compared to the reference devices. In the active layer with Au nanoparticles, the device shows a stronger absorption of the incident light due to the efficient light scattering. Furthermore, the work function of Au or Ag nanoparticles is approximately close to the HOMO energy level of polymer [36, 79]. Considering the difference of energy level, it is possible that the hole transfer occurs from polymer to the nanoparticles, thus resulting in a small energy barrier for hole extraction. Compared with small nanoparticles (about 10 nm), the usage of these large Au nanoparticles (with an average diameter of approximately 70 nm) might also lead to a reduced series resistance because the holes could pass through fewer interfaces to anode (Tables 2, 3).

In conclusion, incorporation of additives to increase the photoabsorption is a simple and promising method to improve the device performance. The additive can

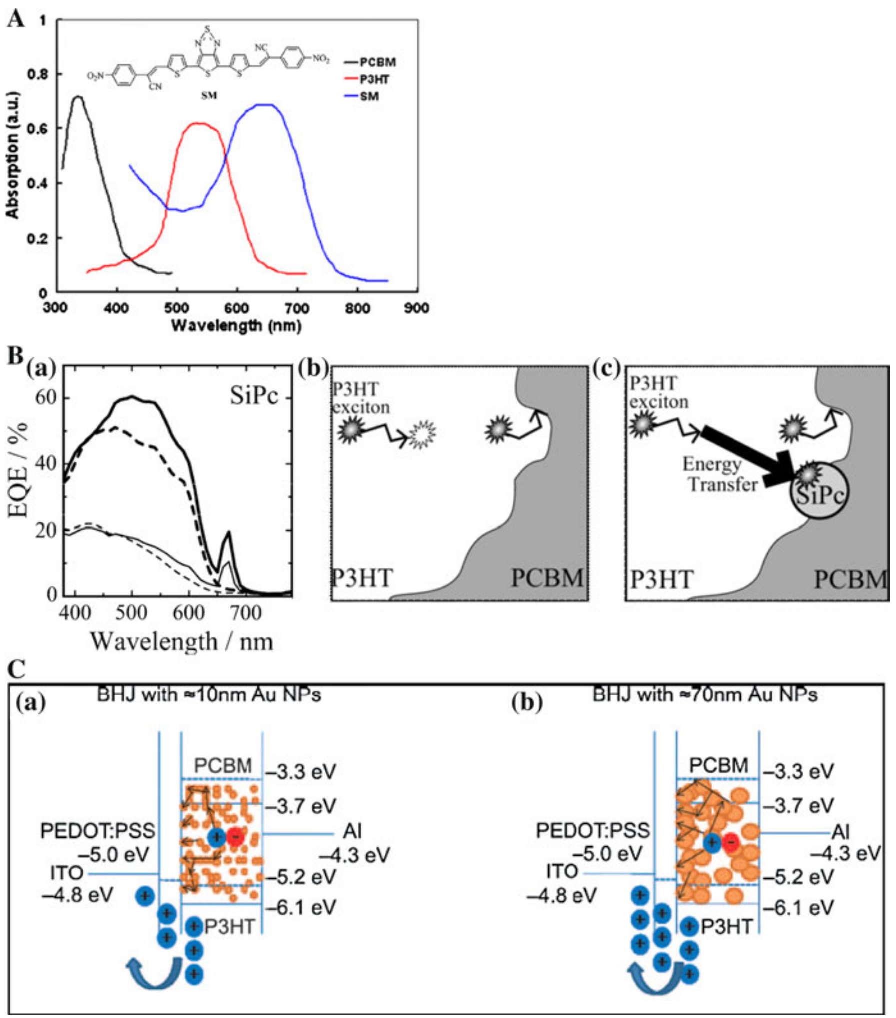

Fig. 5 **A** Optical absorption spectra of PCBM, P3HT and SM, inset shows chemical structures of P3HT, PCBM, and small molecule (SM). Reproduced with permission from Ref. [69]. **B** (*a*) EQE spectra of P3HT/PCBM blend films with (*solid lines*) and without SiPc (*broken lines*) before (*thin lines*) and after annealing (*thick lines*); (*b*) after annealing, some excitons cannot reach the interface because of the larger domain size; (*c*) after annealing and in the presence of SiPc, even excitons generated far away can reach the interface by energy transfer to the SiPc molecule. Reproduced with permission from Ref. [78]. **C** Energy band diagram of photovoltaic devices with Au nanoparticles smaller than 10 nm or larger than the average diameter of 70 nm. (*a*) <10 nm;(*b*) average diameter larger than 70 nm. Reproduced with permission from Ref. [79]

be categorized into three groups: the additives that complement absorption spectra of active layer; the additives have energy transfer to electron donor or acceptor and act as sensitizers; the additives can reflect and scatter light and reduce the series resistance.

Table 2 The device performance with and without additives

System	Additive	J_{sc} (mA/cm^2)	V_{oc} (V)	*FF* (%)	PCE (%)
P3HT/PC$_{61}$BM	ODT [39]				
	Without	1.45	0.65	31	0.29
	With	8.14	0.56	63	2.87
	HDT [45]				
	Without	1.58	0.67	43	0.46
	With	9.38	0.53	64	3.16
PCPDTBT/PC$_{71}$BM	DIO [41]				
	Without	11.74	0.66	43	3.35
	With	15.73	0.61	53	5.12
PBTTPD/PC$_{71}$BM	DIH [42]				
	Without	9.1	0.94	58	5.0
	With	13.1	0.92	61	7.3
P3HT/PC$_{61}$BM	3HT [34]				
	Without	4.22	0.65	52.3	1.43
	With	9.25	0.56	60	3.11
P3HT/PC$_{61}$BM	Transition metal complexes [54]				
	Without	4.51	0.55	39	1.01
	With	6.37	0.54	53	1.81
P3HT/PC$_{61}$BM	SM [69]				
	Without	8.0	0.68	54	2.93
	With	9.2	0.73	55	3.69
	SiPc [78]				
	Without	6.5*	0.58*	59*	2.2*
	With	7.9*	0.58*	59*	2.7*
P3HT/PC$_{61}$BM	DLC [84]				
	Without	0.59*	8.89*	57.39*	3.03*
	With	0.67*	9.15*	64.94*	3.97*

Device with * is characterized after thermal annealing

Change the energy-level distribution and enhance the ordering of P3HT

In order to improve the open circuit voltage and the short-circuit current of the OSCs, the liquid crystal molecules and others such as PPyB are applied to change the energy-level distribution and enhance the ordering of P3HT.

As we know, the V_{oc} of a BHJ solar cell can be estimated by the energy difference between HOMO of donor and LUMO of acceptor. After the addition of liquid molecules, the V_{oc} is improved. This can be explained by a cascade energy-level alignment, since additives exhibit a lower-lying HOMO level compared to P3HT. This larger energy difference ($|E^{\text{additives}}$ HOMO$| - |E^{\text{PCBM}}$ LUMO$|$) at the contact of additive to PCBM may contribute to the increased V_{oc} [84]. In addition to energy-level distribution, the ordering of P3HT is also improved after adding the

Table 3 The category of additive and its function as well as selection principle

Additive	Function	Selection principle
Alkanethiol and diiodoalkane	Enhance the crystallinity and phase separation	(i) Reduce polymer chains entanglement (ii) Have discrepancy in solubility (iii) Have higher boiling point
Aromatic ring molecule and nucleating agent	Enhance the self-organized ability	(i) Have strong chemical affinity (ii) Enhance the coplanar conformation
Hydrophobic molecule	Increase the phase separation	Induce repulsive interactions between donor and acceptor
Amphiphilic molecule	Increase thermal stability	Reduce hydrophilic–hydrophobic repulsive between donor and acceptor
Sensitizer and metal nanoparticles	Improve photon absorption	(i) Complementary absorption spectra (ii) Have energy transfer to electron donor or acceptor (iii) Proper work function and diameter
Liquid crystal molecules	Change energy-level distribution enhance polymer ordering	(i) Proper energy distribution (ii) Strong self-assembling ability

additive [85, 86]. One possible reason is the ordered hexagonal columnar mesophases of DLC induce P3HT packed in an ordered manner. The other might be attributed to the selective solubility of additive in P3HT and $PC_{61}BM$. For example, the NLC additive has a much higher solubility in $PC_{61}BM$ than P3HT, leading to the speculation that the NLC additive selectively exists within the $PC_{61}BM$ domains, which is similar to the processing additive [37]. The $PC_{61}BM$ molecules soluble in NLC additives were able to aggregate during device fabrication, resulting in a phase separation between P3HT and $PC_{61}BM$, which can contribute to the formation of larger $PC_{61}BM$ domains and ordering of P3HT [85].

As a result, the additives change the energy-level distribution and enhance the ordering of P3HT, which would be benefit for the open circuit voltage and the short-circuit current of devices.

The influence of additive on device performance

Adding additive to donor/acceptor blend system could improve the performance of device in efficiency. Different kinds of additives play different roles. The processing additive, aromatic ring molecule or nucleating agent has contribution to the crystallization of polymers and phase separation, which results in an improved J_{sc}. While the amphiphilic molecule could increase the compatibility between donor and acceptor, enhancing the thermal stability of device. The photoelectric properties of active layer also could be adjusted, adding the sensitizer or liquid crystal molecules to blend system can improve the J_{sc} or V_{oc} in efficiency.

Enhance the short-circuit current by crystallization and phase separation

Using alkanethiol and diiodoalkane molecules as additive could improve device performance, which results from an optimized morphology, including the increased crystallinity and proper degree of phase separation. The increased crystallinity favors photon absorption and carrier mobility. Increased phase separation assists formation of interpenetrating networks, which facilitates the charge transport and collection.

The device processed without any additive shows very limited efficiency, often below 1.0%. After the addition of additive, both J_{sc} and FF increase greatly, and PCE is almost several times higher [39, 40]. Adding alkanethiol in P3HT/PC$_{61}$BM, both the J_{sc} and FF increase significantly [40, 45]. Using HDT as additive, J_{sc} increases from 2.3 to 9.1 mA/cm^2, which originates from the optimized photon absorption and the better charge transport. Adding the additive molecules, the crystallinity of polymer is enhanced, resulting in a red shift and increased absorption coefficient. In addition, enhanced carrier lifetime can also be observed [38].This increase in carrier lifetime suggests an improvement in the ratio of shallow traps to deep traps. A proper degree of phase separation also could be obtained. It balances exciton dissociation and charge transport and/or collection, which also favors an improved J_{sc}, and can be confirmed by the increased FF. The photovoltaic cells based on PCPDTBT/PC$_{71}$BM processed with 1,8-diiodooctane as the processing additive also exhibited the highest short-circuit current (15.7 mA/cm^2), the highest fill factor (0.53), and an efficiency that is approximately 50% higher than that obtained without additive [37]. In small band gap polymer:fullerene BHJs, the additive can also raise the yield of photoinduced free carrier formation by suppressing the recombination of photogenerated carrier into the lowest triplet excited state of the polymer [93].

In conclusion, the additive enhances the structural order of polymer and favors a proper degree of phase separation, which facilitates photon absorption and charge transport. Furthermore, in small band gap polymer:fullerene system, the improved charge transport also suppresses the recombination of photogenerated carrier, which result in a several times higher PCE of the device.

Increase the hole mobility by small molecule or nucleating agent

Using aromatic ring molecule or nucleating agent could improve the crystallinity of P3HT in P3HT/PCBM blend system, which results in an increased hole mobility and has a contribution to the increased J_{SC}.

Chang et al. fabricated P3HT/PCBM-based solar cells, the as-cast reference cell performed poorly with V_{OC} of 0.65 V, J_{SC} of 4.22 mA/cm^2, FF of 52.3%, and PCE of 1.43%. In contrast, the 3HT-processed device showed enhanced J_{SC} and FF values of up to 9.25 mA/cm^2 and 60.0%, respectively, with an optimal PCE of 3.11%. The significant increase in J_{SC} is partly originated from the improved hole mobility. In the presence of 3HT, P3HT chains suggest a lower resistance to the hopping of carriers between P3HT backbones. The improved hole mobility also can be observed when adding ATMB as additive. The hole mobility of the hole-only device without ATMB was calculated to be 6.2 × 10^{-5} cm^2/V s, whereas the device with 6 wt% ATMB had a value as high as 6.9 × 10^{-3} cm^2/V s. The hole mobility was two orders of magnitude higher than that of device without ATMB. This result could be attributed partly to the more ordered P3HT chains. The additive acting as nucleating agent also could enhance the hole mobility of the device, in P3HT/PC_{61}BM/$DHPT^3$ based field-effect transistors (FETs) devices, μ_h increases to 1.5 × 10^{-3} cm^2/V s after thermal treatment, while in P3HT/PC_{61}BM reference transistors, μ_h is equal to 7 × 10^{-4} cm^2/V s, which can be attributed to an enhanced structural ordering of P3HT in the presence of $DHPT^3$.

After the addition of aromatic ring molecule or nucleating agent, the crystallinity of P3HT is improved, also result in a smaller interlayer distance between conjugated backbones. This change in morphology is benefit for hole transport.

Form bicontinuous structure or increase thermal stability of device

Adjusting the compatibility between donor and acceptor is a promising way to control the phase separation degree of the active layer. Hydrophobic molecule can be used to induce large domain size that, in turn, form bicontinuous structure. Amphiphilic molecules can be employed to increase the compatibility between donor and acceptor materials, which results in a significant increase in thermal stability of device.

The transition metal complexes, organic salt, and end-functionalized P3HT are used as hydrophobic additive to improve the device performance. Without the additive, the reference device exhibits a PCE of 1.01%, with J_{SC} of 4.51 mA/cm^2, FF of 0.39, and V_{OC} of 0.55 V. After incorporation of additives within the active layer of P3HT and PCBM, the J_{SC} increases. The increased degree is consist with the hydrophobicity of additives, that is to say, the incorporation of most hydrophobic additive (a) yield the highest increase in J_{SC}. Accordingly, the PCE of device with additive (a) increases to 1.81%, an almost twofold increase in device efficiencies compared to reference devices (as shown in Fig. 3B). When F-P3HT is used as additive, J_{SC} is also higher than that of the reference device. In addition, the device fabricated with the F-P3HT blend showed lower series resistance (R_s) and a higher rectification ratio, which are indicative of better charge transport and collection. The improved device performance could be attributed to continuous pathways and a higher crystallinity of P3HT after the addition of additive.

To prevent coarsening of the phase-separated domains upon operation process or thermal annealing, the additive, amphiphilic copolymers, which comprise electron donor and electron acceptor segments have been employed [59, 60, 94]. Using poly(**1**)-*block*-poly(**2**) as additive, thermal stability of the device is improved. Devices fabricated with only P3HT/PC_{61}BM in active layer shows a maximum device efficiency of PCE = 3.1%, while it decreased markedly after extended annealing owing to a large decrease in current density from 8.14 mA/cm^2 for 0.1 h to 7.71 mA/cm^2 for 10 h at 140 °C. The drops of J_{sc} can be illustrated as increased phase segregation, reducing the interfacial area between the two materials. But adding poly(**1**)-*block*-poly(**2**) to the active layer produces devices with a superior thermal stability. After extended thermal treatment, the PCE of the device and its constituent parameters remain essentially unchanged. However, the J_{sc} of these devices are lower than those initially exhibited by the uncompatibilized, reference devices. This reduction in J_{sc} is attributed to the presence of large insulating groups or saturated hydrocarbon backbones in poly(**1**)-*block*-poly(**2**) that ultimately hinder charge separation and transport at the donor/acceptor interface [58]. While thiophene-C_{60} dyads are potential candidates for P3HT/PCBM system, with minimal insulating linker between the electrically active moieties. Of reference devices tested, the J_{sc} of P3HT/PC_{61}BM devices without 4T-C_{60} average of 8.47 ± 0.49 mA/cm^2 after thermal annealing at 170 °C for 1 min. While under the same thermal treatment, the J_{sc} of devices with incorporation of 5 wt% 4T-C_{60} increase to 8.8 ± 0.43 mA/cm^2. This observation indicates that 4T-C_{60} is an effective compatibilizer when added to P3HT and PCBM blends, which is benefit for charge transport and effectively reduces unfavorable contacts between P3HT and PCBM. Thermally annealed photoactive layers in the presence and absence of 4T-C_{60} for extended periods were also carried out. The J_{sc} of reference device decreases significantly from 8.47 ± 0.49 to 6.88 ± 1.92 mA/cm^2 after thermal annealing at 170 °C for 3 h. This variability is directly correlated with the structural heterogeneities that result from macrophase separation of the active layers. Contrary to the reference devices, there is no significant difference in the device with 5 wt% 4T-C_{60} on annealing; the average J_{sc} remained unchanged (as shown in Fig. 4B(b)). This suggests 4T-C_{60} is an effective interfacial agent for compatibilizing blends of P3HT and PCBM in thin films. Its incorporation reduces the interfacial energy between P3HT and PCBM and prevents significant domain coarsening on thermal annealing.

In conclusion, the additives have different influences on device performance. To avoid the thermal annealing treatment, the hydrophobic molecule can be employed to enhance the phase separation, forming interpenetrating structure to facilitate the charge transport. While the application of amphiphilic molecules could prevent coarsening of the phase-separated domains upon operation process or thermal annealing, which improve the thermal stability of device.

Enhance the short-circuit current

The combination of sensitizers and metal nanoparticles with active layer is an effective way to improve light harvesting and has a positive influence on the device performance.

Adding the additives which has complement absorption spectra compared with active layer allows abroad band absorption and would result in an increased J_{sc}. When employed SM [69] as the additive, the band absorption extend from 400 to 780 nm, which leads to an improved PCE value compared with the as-cast device (from 2.93 to 3.69%). This improvement is partly attributed to the enhanced J_{sc}, which results from more photon absorption. Besides the J_{sc}, V_{oc} (0.73 V) of the device with SM is higher than the as-cast device (0.68 V). One possible reason for this might be provided by the energy-level distribution of the P3HT, SM, and PC_{61}BM as mentioned in “Change the energy-level distribution and enhance the ordering of P3HT” section. Using the sensitizers as additive, such as PDI and SiPc, could improve the optical property of some component [77, 78], leading an enhanced J_{sc} of device. Adding SiPc as additive, the

P3HT/$PC_{61}BM$ device exhibits a distinguished increase in J_{sc} from 6.5 to 7.9 mA/cm^2 after the thermal annealing. As a result, the overall device performance is improved. This finding suggests that the appropriate selection of dye molecules is crucial for improving the device performance. The metal nanoparticles can reflect and scatter light and thereby increase the optical path length within the active layer, leading to an improved absorption spectrum [36, 79]. In addition to the photon absorption, another improvement is the reduced series resistances of devices. Using Au nanoparticles with diameter of 70 nm as additive, the series resistances decrease from 1.86 W/cm^2 (without Au) to 1.49 W/cm^2 (with Au) for PCDTBT: $PC_{71}BM$ and from 2.54 W/cm^2 (without Au) to 2.18 W/cm^2 (with Au) for Si-PCPDTBT:$PC_{71}BM$. The reduced series resistance increased the *FF* from 0.64 to 0.65 (PCDTBT: $PC_{71}BM$) and from 0.63 to 0.64 (Si-PCPDTBT: $PC_{71}BM$). In combination of these improvements including the photon absorption and charge transport, for P3HT: $PC_{71}BM$, the PCE increased from 3.54 to 4.36%; for PCDTBT:$PC_{71}BM$, the PCE increased from 5.77 to 6.45%, and for Si-PCPDTBT:$PC_{71}BM$, the PCE increased from 3.92 to 4.54%.

Absorption spectrum is important for high device performance; it can be improved through complementing the absorption spectrum of active layer. After the addition of additives, J_{sc}, *FF* and in some conditions the V_{oc} are improved, which results in a higher device performance.

Enhance the open circuit voltage and the short-circuit current

The addition of additives, such as liquid crystal molecules, would adjust the distribution of energy level in active layers and enhance the ordering of molecules, which are benefit for open circuit voltage and short-circuit current of devices.

When the DLC is employed as additive in P3HT/$PC_{61}BM$ system, the performance of the device is improved. The control device, as-cast without any DLC, presents relatively low device performance after the thermal annealing, with average PCE of 3.03%, $J_{sc} = 8.89$ mA/cm^2, $V_{oc} = 0.59$ V, and $FF = 57.4\%$. While the devices made with DLC additives show considerably enhanced device performances, with an average PCE = 3.97%, with $J_{sc} = 9.15$ mA/cm^2, $V_{oc} = 0.67$ V, and $FF = 64.94\%$. The improved device performance is mainly caused by an increase in V_{oc}, which has been illustrated in the "Improve photon absorption of active layer" section. Except the V_{oc}, DLC also induce improved crystallization of P3HT chains, which is confirmed by the three characteristic absorption peaks of absorption spectra. Moreover, the average crystal size of P3HT is also enlarged, which shows another indication of improved crystallinity. Higher ordering of P3HT chains in the active layer can lead to higher hole mobility. After the thermal annealing, the hole mobility μ_h of the devices without DLC are found to be 1.09×10^{-6} cm^2/V s. However, after the addition of DLC, the μ_h give rise to 8.32×10^{-5} cm^2/V s. Thus, enhanced V_{oc} and increased hole mobility are likely expected to contribute the increased performance of device. While using other molecules, such as PPyB, which has a suit energy-level distribution, a strong self-assembling ability and high charge mobility, also could improve the device performance through the enhanced V_{oc} and increased hole mobility.

In conclusion, the additives used in this system can establish a cascade energy-level alignment between donor and acceptor thus enhanced the V_{oc}. Moreover, a strong self-assembling ability and high charge mobility of the additive improve the charge mobility of hole, resulting in an enhanced J_{sc}. As a result, an improved device performance could be obtained.

Conclusions and outlook

According to the recent researches, modifying the morphology of active layer, enhancing the photoabsorption and increasing the open circuit voltage are all important factors to improve the device performance. Adding additives into active layer is a robust and promising approach to optimize the device performance, which can not only modify the morphology of active layer but also optimize its photoelectric properties, including photon absorption and energy-level distribution. According to the requirement of specific system, proper kind of additive could make up the deficiency, such as unoptimized morphology, poor crystallinity, poor thermal stability, low short-circuit current, and open circuit voltage.

To further improve the device performance, new electron donor and acceptor materials must be carefully designed, for example, energy level and band gap as well as charge transport property should be considered. The development of donor polymers with enhanced optical absorption in red or near infrared part of the solar spectrum is one of the main targets for enhancing cell efficiency. However, it is hard to design a polymer with a low band gap that efficiently absorbs light in the visible spectral region, at the same time maintains a sufficiently low HOMO energy level to insure a high V_{oc}. So, the application of additives which could make up the photon absorption or change energy-level distribution in some specific system is a promising method. In addition, the structure of polymer crystal also has influence on the device performance, such as carrier mobility and photon absorption; as a result, adjusting crystal structure through additive may be an effective way to further improve the device performance. On the base of understanding the mechanism of additive, not only binary but also ternary additives would be employed to improve several aspect of a specific system. Longer term, new additives which posses several functions are required to improve device performance, based on a more detailed understanding of mechanism for controlling the morphology and adjusting the photoelectric properties of BHJ solar cells.

Acknowledgments This study was financially supported by the National Natural Science Foundation of China (20621401, 20834005, and 51073151) and the Ministry of Science and Technology of China (2009CB623604).

References

1. Xue JG (2010) Perspectives on organic photovoltaics. Polym Rev 50:411–419
2. Chen FC, Tseng HC, Ko CJ (2008) Solvent mixtures for improving device efficiency of polymer photovoltaic devices. Appl Phys Lett 92:103316
3. Hoppe H, Sariciftci NS (2004) Organic solar cells: an overview. J Mater Res 19:1924–1945

4. Gunes S, Neugebauer H, Sariciftci NS (2007) Conjugated polymer-based organic solar cells. Chem Rev 107:1324–1338
5. Beaupre S, Breton AC, Dumas J, Leclerc M (2009) Multicolored electrochromic cells based on poly(2,7-carbazole) derivatives for adaptive camouflage. Chem Mater 21:1504–1513
6. Chen HY, Hou JH, Zhang SQ, Liang YY, Yang GW, Yang Y, Yu LP, Wu Y, Li G (2009) Polymer solar cells with enhanced open-circuit voltage and efficiency. Nat Photonics 3:649–653
7. Liang YY, Xu Z, Xia JB, Tsai ST, Wu Y, Li G, Ray C, Yu LP (2010) For the bright future—bulk heterojunction polymer solar cells with power conversion efficiency of 7.4%. Adv Mater 22:E135–E138
8. Chu T-Y, Lu JP, Beaupré S, Zhang YG, Pouliot JR, Wakim S, Zhou JY, Leclerc M, Li Z, Ding JF, Tao Y (2011) Bulk heterojunction solar cells using thieno[3,4-c]pyrrole-4,6-dione and dithieno[3,2-b:20,30-d]silole copolymer with a power conversion efficiency of 7.3%. J Am Chem Soc 133:4250–4253
9. Tang CW (1986) Two-layer organic photovoltaic cell. Appl Phys Lett 48:183–185
10. Marks RN, Halls JJM, Bradley DDC, Friend RH, Holmes AB (1994) The photovoltaic response in poly(*p*-phenylene vinylene) thin-film devices. J Phys: Condens Matter 6:1379–1394
11. Coakley KM, McGehee MD (2004) Conjugated polymer photovoltaic cells. Chem Mater 16: 4533–4542
12. Gregg BA (2003) Excitonic solar cells. J Phys Chem B 107:4688–4698
13. Peumans P, Yakimov A, Forrest SR (2003) Small molecular weight organic thin-film photodetectors and solar cells. J Appl Phys 93:3693–3723
14. Halls JJM, Pichler K, Friend RH, Moratti SC, Holmes AB (1996) Exciton diffusion and dissociation in a poly(p-phenylenevinylene)/C-60 heterojunction photovoltaic cell. Appl Phys Lett 68:3120–3122
15. Theander M, Yartsev A, Zigmantas D, Sundstrom V, Mammo W, Andersson MR, Inganas O (2000) Photoluminescence quenching at a polythiophene/C-60 heterojunction. Phys Rev B 61:12957–12963
16. Sariciftci NS, Braun D, Zhang C, Srdanov VI, Heeger AJ, Stucky G, Wudl F (1993) Semiconducting polymer-buckminsterfullerene heterojunctions-diodes, photodiodes, and photovoltaic cells. Appl Phys Lett 62:585–587
17. Yu G, Heeger AJ (1995) Charge separation and photovoltaic conversion in polymer composites with internal donor–acceptor heterojunctions. J Appl Phys 78:4510–4515
18. Halls JJM, Walsh CA, Greenham NC, Marseglia EA, Friend RH, Moratti SC, Holmes AB (1995) Efficient photodiodes from interpenetrating polymer networks. Nature 376:498–500
19. Hill IG, Kahn A, Soos ZG, Pascal RA (2000) Charge-separation energy in films of pi-conjugated organic molecules. Chem Phys Lett 327:181–188
20. Barth S, Bassler H (1997) Intrinsic photoconduction in PPV-type conjugated polymers. Phys Rev Lett 79:4445–4448
21. Forrest SR (2005) The limits to organic photovoltaic cell efficiency. MRS Bull 30:28–32
22. Li G, Shrotriya V, Huang JS, Yao Y, Moriarty T, Emery K, Yang Y (2005) High-efficiency solution processable polymer photovoltaic cells by self-organization of polymer blends. Nat Mater 4:864–868
23. Yang XN, van Duren JKJ, Janssen RAJ, Michels MAJ, Loos J (2004) Morphology and thermal stability of the active layer in poly(*p*-phenylenevinylene)/methanofullerene plastic photovoltaic devices. Macromolecules 37:2151–2158
24. Shaheen SE, Brabec CJ, Sariciftci NS, Padinger F, Fromherz T, Hummelen JC (2001) 2.5% efficient organic plastic solar cells. Appl Phys Lett 78:841–843
25. Zhao Y, Xie ZY, Qu Y, Geng YH, Wang LX (2007) Solvent-vapor treatment induced performance enhancement of poly(3-hexylthiophene): methanofullerene bulk-heterojunction photovoltaic cells. Appl Phys Lett 90:043504
26. Zhao Y, Guo XY, Xie ZY, Qu Y, Geng YH, Wang LX (2009) Solvent vapor-Induced self assembly and its influence on optoelectronic conversion of poly(3-hexylthiophene): methanofullerene bulk heterojunction photovoltaic cells. J Appl Polym Sci 111:1799–1804
27. Ko CJ, Lin YK, Chen FC (2007) Microwave annealing of polymer photovoltaic devices. Adv Mater 19:3520–3523
28. Yang XN, Loos J, Veenstra SC, Verhees WJH, Wienk MM, Kroon JM, Michels MAJ, Janssen RAJ (2005) Nanoscale morphology of high-performance polymer solar cells. Nano Lett 5:579–583
29. Chirvase D, Parisi J, Hummelen JC, Dyakonov V (2004) Influence of nanomorphology on the photovoltaic action of polymer-fullerene composites. Nanotechnology 15:1317–1323
30. Erb T, Zhokhavets U, Gobsch G, Raleva S, Stuhn B, Schilinsky P, Waldauf C, Brabec CJ (2005) Correlation between structural and optical properties of composite polymer/fullerene films for organic solar cells. Adv Funct Mater 15:1193–1196

31. Mihailetchi VD, Xie HX, de Boer B, Koster LJA, Blom PWM (2006) Charge transport and photocurrent generation in poly(3-hexylthiophene): methanofullerene bulk-heterojunction solar cells. Adv Funct Mater 16:699–708
32. Brabec CJ, Heeney M, McCulloch I, Nelson J (2011) Influence of blend microstructure on bulk heterojunction organic photovoltaic performance. Chem Soc Rev 40:1185–1199
33. Berson S, De Bettignies R, Bailly S, Guillerez S (2007) Poly (3-hexylthiophene) fibers for photovoltaic applications. Adv Funct Mater 17:1377–1384
34. Chang YM, Wang L (2008) Efficient poly(3-hexylthiophene)-based bulk heterojunction solar cells fabricated by an annealing-free approach. J Phys Chem C 112:17716–17720
35. Koppe M, Brabec CJ, Heiml S, Schausberger A, Duffy W, Heeney M, McCulloch I (2009) Influence of molecular weight distribution on the gelation of P3HT and its impact on the photovoltaic performance. Macromolecules 42:4661–4666
36. Kim K, Carroll DL (2005) Roles of Au and Ag nanoparticles in efficiency enhancement of poly(3-octylthiophene)/C-60 bulk heterojunction photovoltaic devices. Appl Phys Lett 87:203113
37. Lee JK, Ma WL, Brabec CJ, Yuen J, Moon JS, Kim JY, Lee K, Bazan GC, Heeger AJ (2008) Processing additives for improved efficiency from bulk heterojunction solar cells. J Am Chem Soc 130:3619–3623
38. Peet J, Soci C, Coffin RC, Nguyen TQ, Mikhailovsky A, Moses D, Bazan GC (2006) Method for increasing the photoconductive response in conjugated polymer/fullerene composites. Appl Phys Lett 89:252105
39. Yao Y, Hou JH, Xu Z, Li G, Yang Y (2008) Effect of solvent mixture on the nanoscale phase separation in polymer solar cells. Adv Funct Mater 18:1783–1789
40. Liu JG, Shao SY, Wang HF, Zhao K, Xue LJ, Gao X, Xie ZY, Han YC (2010) The mechanisms for introduction of *n*-dodecylthiol to modify the P3HT/PCBM morphology. Org Electron 11:775–783
41. Peet J, Kim JY, Coates NE, Ma WL, Moses D, Heeger AJ, Bazan GC (2007) Efficiency enhancement in low-bandgap polymer solar cells by processing with alkane dithiols. Nat Mater 6:497–500
42. Su M-S, Kuo C-Y, Yuan M-C, Jeng US, Su C-J, Wei K-H (2011) Improving device efficiency of polymer/fullerene bulk heterojunction solar cells through enhanced crystallinity and reduced grain boundaries induced by solvent additives. Adv Mater 23:3315–3319
43. Yang X, Loos J (2007) Toward high-performance polymer solar cells: the importance of morphology control. Macromolecules 40:1353–1362
44. Bavel SSv, Sourty E, With Gd (2009) Three-dimensional nanoscale organization of bulk heterojunction polymer solar cells. Nano Lett 9:507–513
45. Salim T, Wong LH, Brauer B, Kukreja R, Foo YL, Bao ZN, Lam YM (2011) Solvent additives and their effects on blend morphologies of bulk heterojunctions. J Mater Chem 21:242–250
46. Rughooputh S, Hotta S, Heeger AJ, Wudl F (1987) Chromism of soluble polythienylenes. J Polym Sci B 25:1071–1078
47. Colby RH, Rubinstein M, Viovy JL (1992) Chain entanglement in polymer melts and solutions. Macromolecules 25:996–998
48. Jeong S, Woo SH, Lyu HK, Han YS (2011) Effects of a perfluorinated compound as an additive on the power conversion efficiencies of polymer solar cells. Sol Energy Mater Sol Cells 95:1908–1914
49. Barrau S, Zhang F, Herland A, Mammo W, Andersson MR, Inganas O (2008) Integration of amyloid nanowires in organic solar cells. Appl Phys Lett 93:023307
50. Yin C, Shen XY (2005) Thermal property of super bright polyester chips. J Textile Res 26:86–87
51. Telkes M (1952) Nucleation of supersaturated inorganic salt solutions. Ind Eng Chem 44:1308–1310
52. Bechara R, Leclerc N, Léve Que P, Richard F, Heiser T, Hadziioannou G (2008) Efficiency enhancement of polymer photovoltaic devices using thieno-thiophene based copolymers as nucleating agents for polythiophene crystallization. Appl Phys Lett 93:013306
53. Kim JY, Frisbie D (2008) Correlation of phase behavior and charge transport in conjugated polymer/fullerene blends. J Phys Chem C 112:17726–17736
54. Kim CS, Tinker LL, DiSalle BF, Gomez ED, Lee S, Bernhard S, Loo YL (2009) Altering the thermodynamics of phase separation in inverted bulk-heterojunction organic solar cells. Adv Mater 21:3110–3115
55. Lim B, Jo J, Na SI, Kim J, Kim SS, Kim DY (2010) A morphology controller for high-efficiency bulk-heterojunction polymer solar cells. J Mater Chem 20:10919–10923
56. Peumans P, Uchida S, Forrest SR (2003) Efficient bulk heterojunction photovoltaic cells using small-molecular-weight organic thin films. Nature 425:158–162

57. Zen A, Saphiannikova M, Neher D, Grenzer J, Grigorian S, Pietsch U, Asawapirom U, Janietz S, Scherf U, Lieberwirth I, Wegner G (2006) Effect of molecular weight on the structure and crystallinity of poly(3-hexylthiophene). Macromolecules 39:2162–2171
58. Kim JB, Allen K, Oh SJ, Lee S, Toney MF, Kim YS, Kagan CR, Nuckolls C, Loo YL (2010) Small-molecule thiophene-C-60 dyads as compatibilizers in inverted polymer solar cells. Chem Mater 22:5762–5773
59. Zhang QL, Cirpan A, Russell TP, Emrick T (2009) Donor–acceptor poly(thiophene-*block*-perylene diimide) copolymers: synthesis and solar cell fabrication. Macromolecules 42:1079–1082
60. Tao Y, McCulloch B, Kim S, Segalman RA (2009) The relationship between morphology and performance of donor–acceptor rod–coil block copolymer solar cells. Soft Matter 5:4219–4230
61. Sivula K, Ball ZT, Watanabe N, Frechet JMJ (2006) Amphiphilic diblock copolymer compatibilizers and their effect on the morphology and performance of polythiophene: fullerene solar cells. Adv Mater 18:206–210
62. Lindner SM, Thelakkat M (2004) Nanostructures of n-type organic semiconductor in a p-type matrix via self-assembly of block copolymers. Macromolecules 37:8832–8835
63. van der Veen MH, de Boer B, Stalmach U, van de wetering KI, Hadziioannou G (2004) Donor–acceptor diblock copolymers based on PPV and C-60: synthesis, thermal properties, and morphology. Macromolecules 37:3673–3684
64. Zhu Z, Waller D, Gaudiana R, Morana M, Muhlbacher D, Scharber M, Brabec C (2007) Panchromatic conjugated polymers containing alternating donor/acceptor units for photovoltaic applications. Macromolecules 40:1981–1986
65. Blouin N, Michaud A, Leclerc M (2007) A low-bandgap poly(2,7-carbazole) derivative for use in high-performance solar cells. Adv Mater 19:2295–2300
66. Kooistra FB, Knol J, Kastenberg F, Popescu LM, Verhees WJH, Kroon JM, Hummelen JC (2007) Increasing the open circuit voltage of bulk-heterojunction solar cells by raising the LUMO level of the acceptor. Org Lett 9:551–554
67. Kim JY, Lee K, Coates NE, Moses D, Nguyen TQ, Dante M, Heeger AJ (2007) Efficient tandem polymer solar cells fabricated by all-solution processing. Science 317:222–225
68. He Z, Zhong C, Huang X, Wong W-Y, Wu H, Chen L, Su S, Cao Y (2011) Simultaneous enhancement of open-circuit voltage, short-circuit current density, and fill factor in polymer solar cells. Adv Mater. doi: 10.1002/adma.201103006
69. Sharma SS, Sharma GD, Mikroyannidis JA (2011) Improved power conversion efficiency of bulk heterojunction poly(3-hexylthiophene):PCBM photovoltaic devices using small molecule additive. Sol Energy Mater Sol Cells 95:1219–1223
70. Peet J, Tamayo AB, Dang XD, Seo JH, Nguyena TQ (2008) Small molecule sensitizers for near-infrared absorption in polymer bulk heterojunction solar cells. Appl Phys Lett 93:163306
71. Xu Z-X, Roy VAL, Low K-H, Che C-M (2011) Bulk heterojunction photovoltaic cells based on tetra-methyl substituted copper(ii) phthalocyanine:P3HT:PCBM composite. Chem Commun 47:9654–9656
72. Mihailetchi VD, van Duren JKJ, Blom PWM, Hummelen JC, Janssen RAJ, Kroon JM, Rispens MT, Verhees WJH, Wienk MM (2003) Electron transport in a methanofullerene. Adv Funct Mater 13:43–46
73. He Y, Chen H-Y, Hou J, Li Y (2010) Indene-C(60) bisadduct: a new acceptor for high-performance polymer solar cells. J Am Chem Soc 132:1377–1382
74. Schmidt-Mende L, Fechtenkotter A, Mullen K, Moons E, Friend RH, MacKenzie JD (2001) Self-organized discotic liquid crystals for high-efficiency organic photovoltaics. Science 293:1119–1122
75. Anthony JE (2011) Nonfullerene acceptors for polymer bulk heterojunction organic photovoltaics. Chem Mater 23:583–590
76. Hesse HC, Weickert J, Al-Hussein M, Dössel L, Feng X, Müllen K, Schmidt-Mende L (2010) Discotic materials for organic solar cells: effects of chemical structure on assembly and performance. Sol Energy Mater Sol Cells 94:560–567
77. Hesse HC, Weickert J, Hundschell C, Feng X, Müllen K, Nickel B, Mozer AJ, Schmidt-Mende L (2011) Perylene sensitization of fullerenes for improved performance in organic photovoltaics. Adv Mater. doi:10.1002/aenm.201100211
78. Honda S, Nogami T, Ohkita H, Benten H, Ito S (2009) Improvement of the light-harvesting efficiency in polymer/fullerene bulk heterojunction solar cells by interfacial dye modification. ACS Appl Mater Interfaces 1:804–810

79. Wang DH, Kim DY, Choi KW, Seo JH, Im SH, Park JH, Park OO, Heeger AJ (2011) Enhancement of donor–acceptor polymer bulk heterojunction solar cell power conversion efficiencies by addition of Au nanoparticles. Angew Chem Int Ed 50:5519–5523
80. Konda RB, Mundle R, Mustafa H, Bamiduro O, Pradhan AK, Roy UN, Cui Y, Burger A (2007) Surface plasmon excitation via Au nanoparticles in n-CdSe/p-Si heterojunction diodes. Appl Phys Lett 91:191111
81. Koster LJA, Mihailetchi VD, Blom PWM (2006) Ultimate efficiency of polymer/fullerene bulk heterojunction solar cells. Appl Phys Lett 88:093511
82. Scharber MC, Wuhlbacher D, Koppe M, Denk P, Waldauf C, Heeger AJ, Brabec CL (2006) Design rules for donors in bulk-heterojunction solar cells—towards 10 % energy-conversion efficiency. Adv Mater 18:789–794
83. Blouin N, Michaud A, Gendron D, Wakim S, Blair E, Neagu-Plesu R, Belletete M, Durocher G, Tao Y, Leclerc M (2008) Toward a rational design of poly(2,7-carbazole) derivatives for solar cells. J Am Chem Soc 130:732–742
84. Jeong S, Kwon Y, Choi BD, Ade H, Han YS (2010) Improved efficiency of bulk heterojunction poly(3-hexylthiophene):[6,6]-phenyl-C-61-butyric acid methyl ester photovoltaic devices using discotic liquid crystal additives. Appl Phys Lett 96:183305
85. Jeong S, Kwon Y, Choi BD, Kwak G, Han YS (2010) Effects of nematic liquid crystal additives on the performance of polymer solar cells. Macromol Chem Phys 211:2474–2479
86. Canli NY, Gunes S, Pivrikas A, Fuchsbauer A, Sinwel D, Sariciftci NS, Yasa O, Bilgin-Eran B (2010) Chiral (*S*)-5-octyloxy-2-[{4-(2-methylbuthoxy)-phenylimino}-methyl]-phenol liquid crystalline compound as additive into polymer solar cells. Sol Energy Mater Sol Cells 94:1089–1099
87. Jeong S, Han YS, Kwon Y, Choi MS, Cho G, Kim KS, Kim Y (2010) Effects of n-type perylene derivative as an additive on the power conversion efficiencies of polymer solar cells. Synth Met 160:2109–2115
88. van de Craats AM, Warman JM, Fechtenkotter A, Brand JD, Harbison MA, Mullen K (1999) Record charge carrier mobility in a room-temperature discotic liquid-crystalline derivative of hexabenzocoronene. Adv Mater 11:1469–1472
89. Wang WL, Wu HB, Yang CY, Luo C, Zhang Y, Chen JW, Cao Y (2007) High-efficiency polymer photovoltaic devices from regioregular-poly(3-hexylthiophene-2,5-diyl) and [6,6]-phenyl-C-61-butyric acid methyl ester processed with oleic acid surfactant. Appl Phys Lett 90:183512
90. Kircher T, Löhmannsröben HG (1999) Photoinduced charge recombination reactions of a perylene dye in acetonitrile. PCCP 1:3987–3992
91. Stenzel O, Lebedev AN, Schreiber M, Zahn DRT (2000) Simulation of linear optical losses of absorbing heterogeneous thin solid films. Thin Solid Films 372:200–208
92. Soon YW, Clarke TM, Zhang W, Agostinelli T, Kirkpatrick J, Dyer-Smith C, McCulloch I, Nelson J, Durrant JR (2011) Energy versus electron transfer in organic solar cells: a comparison of the photophysics of two indenofluorene:fullerene blend films. Chem Sci 2:1111–1120
93. Di Nuzzo D, Aguirre A, Shahid M, Gevaerts VS, Meskers SCJ, Janssen RAJ (2010) Improved film morphology reduces charge carrier recombination into the triplet excited state in a small bandgap polymer-fullerene photovoltaic cell. Adv Mater 22:4321–4324
94. Yang C, Lee JK, Heeger AJ, Wudl F (2009) Well-defined donor–acceptor rod–coil diblock copolymers based on P3HT containing C(60): the morphology and role as a surfactant in bulk-heterojunction solar cells. J Mater Chem 19:5416–5423